

Structural Depth Studies

Solutions that are presented in this portion of the report are in response to the problem statement and design criteria as stated. The structural redesigns presented herein have been designed with many simplifying assumptions as to expedite the analysis and design process and not compromise the integrity of this year long study. The goal of the structural redesign is to replace the current reinforced concrete shear wall core with a core of braced frames. This includes the redesign of the current filigree flat plate floor system as a steel frame with precast concrete planks. The overall design of the steel system will be ultimately compared to the current concrete system. Conclusions will be based upon performance, cost, schedule, architectural impacts, and construction impacts.

Material Strength Specifications

Unless otherwise noted, the following grades and material strengths will be used for the redesigned structural components from here within:

Structural Steel W-Shapes.....	A992
Structural Plates and Angles.....	A36
Built-up Section Plates.....	A572-Gr 50
Bolts (Basic Beam to Girder Connections).....	3/4" - A490N
Bolts (Column Splices and Girder to Column Connections).....	3/4" – A490 Slip Critical
Shear Studs.....	3/4" – ASTM A108
Anchor Bolts.....	A449-Gr 120
Topping Slab 28 Day Strength.....	3000psi
Mat Foundation 28 Day Strength.....	5000psi
Precast Plank Prestressing Strands.....	0.6"Φ270ksi Lo-Relaxation
Precast Plank 28 Day Strength.....	6000psi

Gravity System Redesign

Introduction

The proposed gravity system redesign consists of replacing the filigree flat plate system with a non-composite steel frame with precast plank and topping slab. This type of system was chosen due to its superior erection time and cost savings, the main goals of this study are such.

Methodology

This system utilizes precast pre-stressed hollow core concrete planks as the floor slab and steel girders as

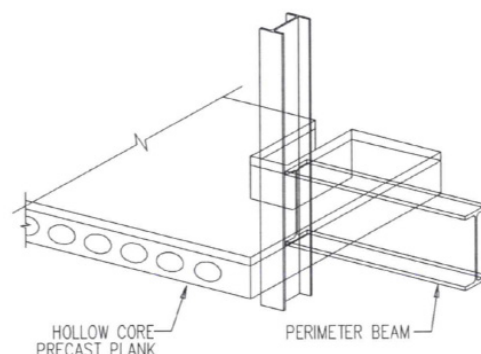


Figure 20: Precast Plank and Steel Frame Isometric Diagram



supports. Precast planks with a 2" topping span the length of the floor, transferring the floor load to the steel W-shape girders. The girders then transfer the load to W-14 steel columns. Finally, the load is transferred from the columns to the mat foundation.

The 2" topping slab is required for both fire protection and floor leveling purposes, but it is also necessary to provide an adequate bond between the planks to ensure that the floor system acts as a rigid diaphragm under lateral loading. Because precast planks were chosen as the floor system, a composite steel frame was not an option and a non-composite steel frame was used. A non-composite steel frame is not able to utilize the compressive strength of a concrete slab; therefore the members are often heavier and/or deeper.

Design Goals and Assumptions

The overall design goal is to convert the current filigree flat plate system with a non-composite steel frame and precast plank floor system. Other goals and assumptions are as follows:

Design Goals

- Develop a steel framing plan that adequately meets the requirements of the Trump Taj Mahal Hotel without causing alterations to the architecture of the tower.
- Develop a floor system that utilizes the strength of the precast planks efficiently.
- Limit member depths as to not interfere with the architecture and mechanical requirements of the Trump Taj Mahal Hotel.
- Develop a RAM Steel model in input live and dead loads to obtain steel sizes that conform to the strength and serviceability requirement of both ASCE 7-05 and AISC Manual of Steel Construction 13th Edition LRFD.
- Beam deflection shall be limited to $L/240$ for dead + live load, $L/360$ for live load, and $1/2$ " for spandrel beams per curtain wall requirements.
- Check over RAM Steel designs and optimize design by using similar W-shapes.
- Spot check a typical exterior girder to verify RAM designs.
- Develop typical details of the non-composite steel frame with precast plank system.

Design Assumptions

- Columns will be braced by not only steel framing, but precast concrete planks as well; this detail was verified by a representative of Nitterhouse, Inc.
- The sign structure at the top of the tower has been omitted for simplicity.
- Elevator and stair framing has not been designed due to unknown load requirement. Cost will be considered based on the design of the structural engineer of record.
- Additional bracing and design requirements for the torsional resistance of spandrel beams have not been accounted for. Numerous design solutions exist, however impact towards cost and schedule will not be impacted enough to merit consideration for this study.



Design Process

The initial design process began with countless hours of sketching, delicately placing steel framing as to not inhibit the architecture or mechanical systems of the tower. Both typical tower levels and atypical levels of the tower were framed. Upon completing the steel framing layout, the precast planks were designed for the longest span and loading for a typical floor of the tower. Planks were designed using the loading tables provided by Nitterhouse, Inc. The planks of atypical levels were also verified to meet strength requirements. Calculations and loading tables can be found in Appendix B.

After completing the framing layout and plank design, a RAM Steel model was created to size steel members. RAM was used because it is widely recognized in practice as one of the best steel gravity design and analysis programs. Layouts of all floors of the tower were created, including atypical levels. Dead and live loads were input into the RAM model, live load reduction in accordance with ASCE 7-05 and model code IBC 2003 were incorporated for column design only. A linear load to account for the weight of the curtain wall was placed along the perimeter of the diaphragm. Again, spandrel beams were not designed for torsion for simplification purposes. Snow loads were calculated per ASCE 7-05; however for simplicity drifting was not a consideration as it poses little ramifications to the overall cost of the frame. As a small note, the 10" floor to floor height increase has been taken into account prior to the design of the steel frame.

Upon completion of the model layout, the model was run in order to obtain steel designs. Girders were not cambered in order to accommodate easier connection constructability. All members were reviewed and sized by the user according to repetitive member selection, connection constructability (i.e. beams were not permitted to be deeper than girders), and depth restrictions imposed by mechanical and architectural requirements. The results of the steel gravity design for a typical bay and the core are shown below in Figure 23 and Figure 24, respectively. Framing plans and member sizes for all levels of the tower can be found in Appendix B.

Typical details of the framing system were developed to illustrate plank connections to the steel frame. These details are important in understanding the load path of both the gravity and lateral loads, as well as getting a sense of how the system is constructed.

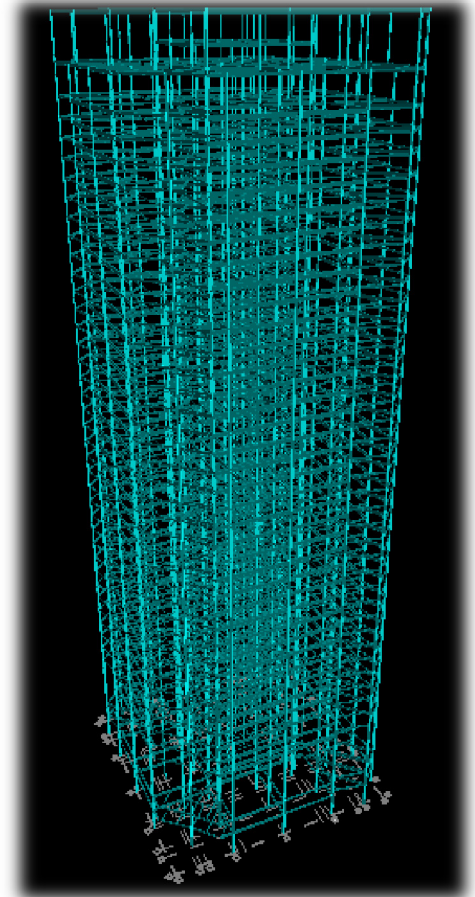


Figure 21: 3D RAM Model Isometric



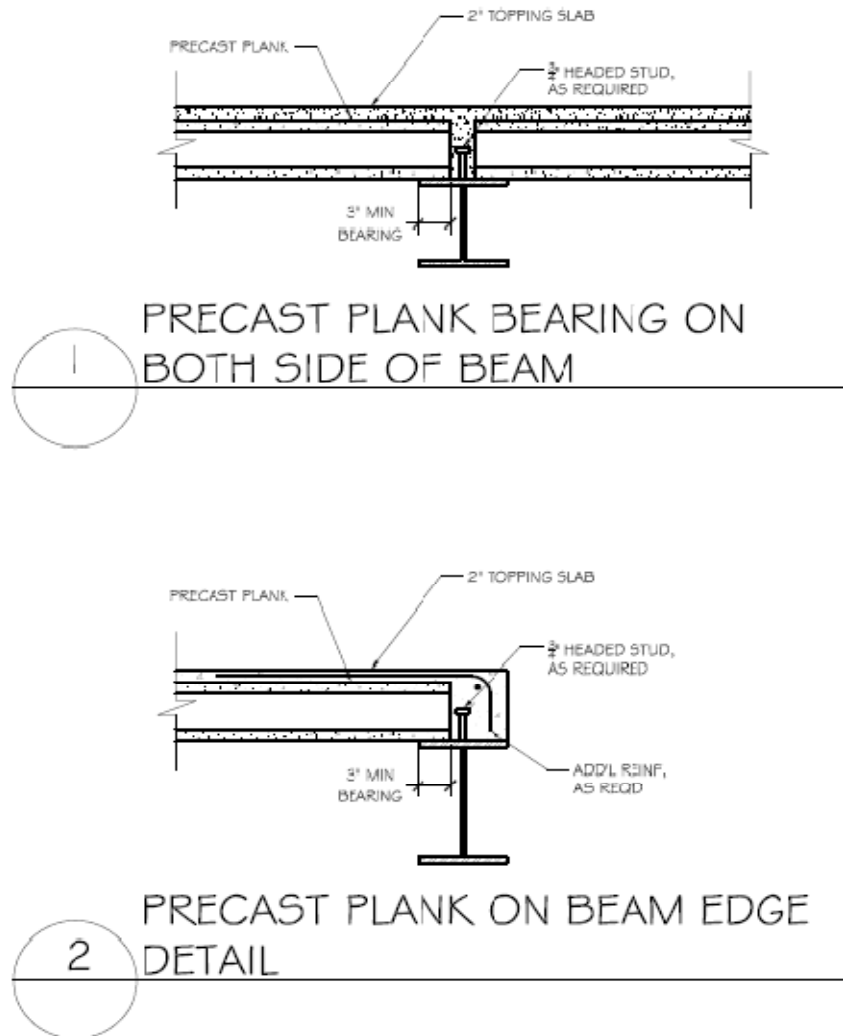


Figure 22: Non-Composite Steel Frame with Precast Plank Details
Note: Shear Studs Provided for Transfer of Lateral Loads

After completing the beam design, the steel columns were designed. Columns were designed on the basis that weak and strong axis buckling would be fully restrained by both steel framing members as well as the precast concrete planks and topping. Columns were typically spliced every 4 levels to accommodate faster steel erection. This results in approximately 42' long steel columns. Column splices will be discussed further in the construction management breadth of this study. All column sizes can be found in Appendix B.

The weight of each floor was calculated by RAM Frame. Each floor approximately weighs 2000 kips. This weight can be converted to a unit mass for input into ETABS by:



$$\text{Mass Per Unit Area} = \frac{\text{Wt. of Floor (kips)} \times 1000 \text{ lbs/kip}}{389 \text{ in/sec}^2 \times \text{Floor Area (in}^2\text{)}} \quad \text{Equation 1}$$

This mass will be applied to the ETABS model per unit area for lateral dynamic analysis purposes. For a typical floor with an area of 2421520.9 in², this mass translates to 1.9x10⁶ lb-sec² /in³.

The factor of safety against overturning of the building can now be calculated since the weight of the structure is known. Using the most sever wind tunnel test overturning moment of 1,048,568 ft-kips and a resisting moment of 6,190,260 ft-kips, the factor of safety is determined by:

$$\text{F.S.} = \frac{\text{Resisting Moment}}{\text{Overturning Moment}} \quad \text{Equation 2}$$

This results in a factor of safety of 6.7 and is more than two times greater than the recommended factor of safety is 3.0; therefore overturning is not a stability issue. Calculations are available upon request.

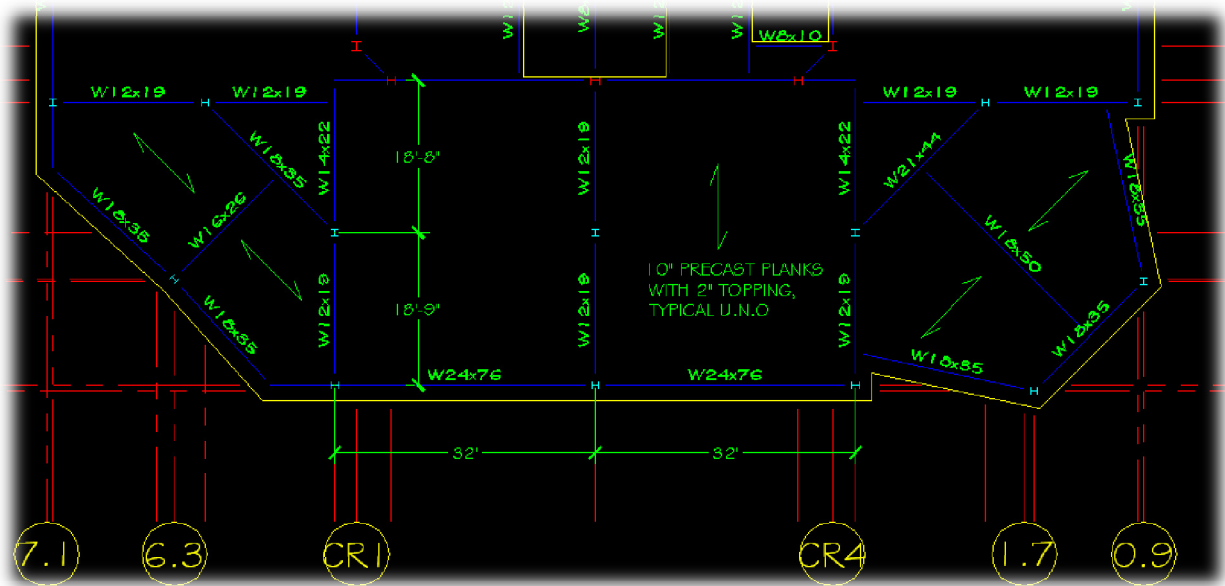


Figure 23: Typical Bay Steel Frame and Plank Framing Plan



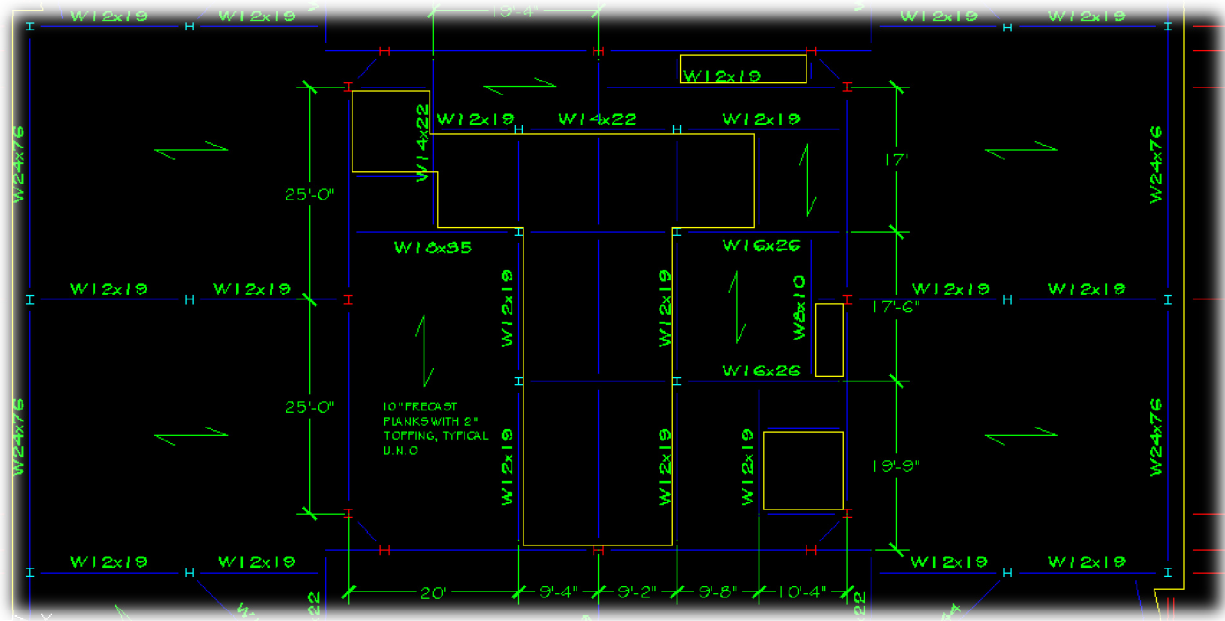


Figure 24: Typical Core Steel Frame and Plank Framing Plan



Braced Frame Core Design

Introduction

The proposed lateral force resisting system redesign consist of replacing the core of concrete shear walls with braced frames as seen in Figure 25 and 26, respectively. A steel braced frame was chosen to be evaluated due to the stiffness that can be provided to the building in such a small amount of space. Braced frames are often preferred over moment frames because moment frames offer construction challenges in terms of field connections; which translates to higher cost.

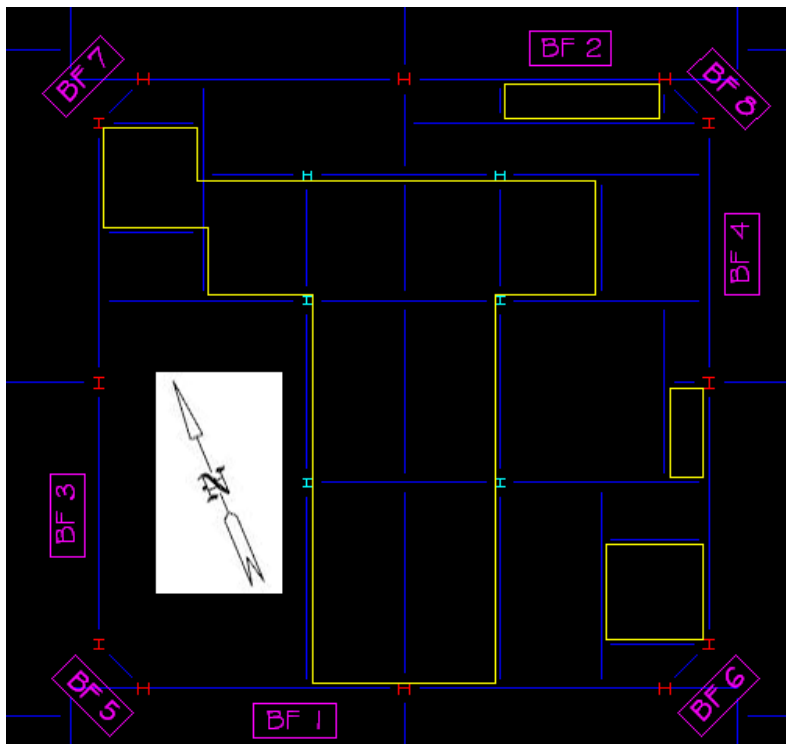


Figure 25: Plan Layout of the Braced Frame Core

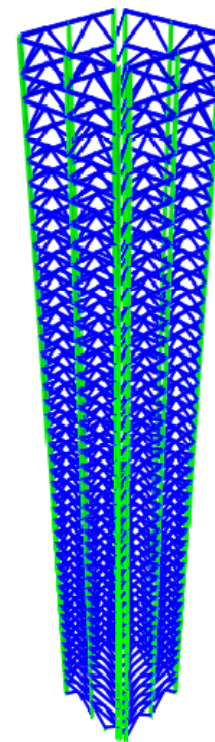


Figure 26: ETABS Isometric of Braced Frame Core

Initial member sizes of the braced frames were determined using classical, simplified methods. These initial sizes were input into an ETABS model for further design and optimization. Design groups were chosen at every 8 floors (a total of 5 design groups) for simplification. Results of the analysis and optimization will meet the requirements of code and the recommended drift limitation of $H/400$. Braced frame connections shall be detailed and designed in a simplified manner to illustrate feasibility. The punching shear of the mat foundation will be evaluated to assure that an increase in mat thickness will not be required; or conversely to see if a decrease in thickness is feasible. Finally, a parametric acceleration check will be performed following the procedure presented in *Serviceability Limit States under Wind Load*, by Lawrence G. Griffis. Acceleration is often an issue with tall, slender, core-only steel structures.



This is a serviceability issue and is related to the motion perception of the building occupants at the upper levels of the tower.

Before any design was conducted, the layout of the elevator and service core was changed to accommodate the braced frame core. Openings were moved and areas were redesigned accordingly as to provide as many concentrically braced frames as possible. Concentrically braced frames are preferred over eccentrically braced frames because a concentrically braced frame provides greater stiffness to the overall structure. Eccentrically braced frames were avoided as much as possible, but were still required at the elevator lobbies of the core to accommodate the opening. For a more detailed core layout analysis, see the architectural breadth of this report.

Methodology

A braced frame is an extremely efficient system because the horizontal shear forces resulting from lateral loads are resisted by the axial capacities of the braces and columns of the system. The system effectively acts as a vertical truss, where little or no moment exists in the columns, beams, or braces. Since forces are resisted mostly by axial forces, a highly efficient system results because the complete cross section of steel section resists the forces, compared to just the deformations caused by bending.

Before a design procedure can be set forth, it is important to understand the behavior of such a braced frame system. After conducting independent research while speaking with various design professionals, it was found that the exterior columns of the braced frame convert the bending forces of the system into axial tension and compression, while the braces convert the shear forces of the system into axial tension and compression. This type of behavior is analogous to a wide flange beam, where the columns of the braced frame act as the flange and the braces as the web. The interior columns act as “zipper columns” and resist little axial forces caused by lateral loads. Zipper columns act more as intermediate supports for girders and brace. This behavior is illustrated in Figure 27.

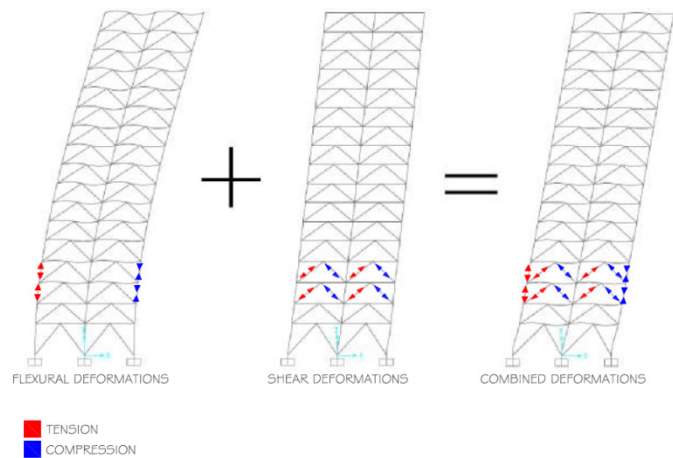


Figure 27: Braced Frame Behavior

Columns in the braced frame of tall buildings accumulate large axial forces from both lateral and gravity loads. These forces result in large axial deformations in the columns. In the braced frame of a tall building, a large percentage of the building drift results from the deformations in the columns, known as “chord drift”. A smaller percentage of the building drift results from the shear deformations of the braces, known as “shear racking”. Because columns play a pivotal role in the control of drift, large columns are often necessary to control the accumulating shear and gravity forces of the building. This will result in a large column size that is often in excess of the strength requirement.



Design Goals and Assumptions

The overall design goal of this redesign is to effectively replace the concrete shear wall core with a core of braced frames. Other goals are as follows:

Design Goals

- Obtain initial column sizes based upon the simplified moment area method.
- Obtain and compare initial sizes of moment area method with the virtual work method provided in AISC Design Guide 5 – Design of Low and Medium Rise Buildings.
- Setup ETABS model with initial frame layouts and member designs.
- Input wind tunnel test and ASCE 7-05 seismic design loads into ETABS model.
- Run ETABS model and iterate design groups until strength and drift criteria has been satisfied.
- Provide an optimal braced frame design for use in further investigation.
- Spot and hand check critical columns, braces, and girders.
- Design and detail the typical braced frame connections.
- Design the most critical braced frame column base plate.

In order to expedite the design process, a few assumptions were made. These assumptions are as follows:

Design Assumptions

- To obtain initial trial sizes, forces were distributed evenly among frames.
- Wind loads determined according to ASCE 7-05 MWFRS were neglected and only the loads of the wind tunnel test were used.
- Columns, braces, and girders are designed by groups, 8 floors in each group for a total of 5 design groups.
- P-delta effects were considered in the drift and strength design.
- Rigid diaphragm action results from the precast planks with 2” concrete topping. However, semi-rigid diaphragm action was used in order to impose axial forces on the girders of the braced frame.
- Concentric inverted “V” Chevron braces will be utilized whenever possible, as they provide greater stiffness over eccentric braces.
- Lumped mass was applied to each diaphragm over the entire area of the diaphragm. These masses were found using the RAM Steel output.

Design Process

To gauge the initial member sizes of the braced frames, two classical methods of analysis were utilized. Moment area method and the virtual work method presented in AISC Design Guide 5 were used to obtain initial column, brace, and girder sizes. Both methods neglect the impacts of gravity loads.



Moment area method

Moment area method assumes that all of the deformations of the braced frame are due to flexure and the cross section of the end columns resist the tension and compression forces caused by bending. The flexure forces result from the overturning moments caused by the wind tunnel loads, where the most extreme loads were taken. It is important to note that both the effects of torsion and gravity are neglected by moment area method. Also, it is assumed that each brace contributes equally to the resistance of the lateral loads. Detailed calculations can be found in Appendix C.

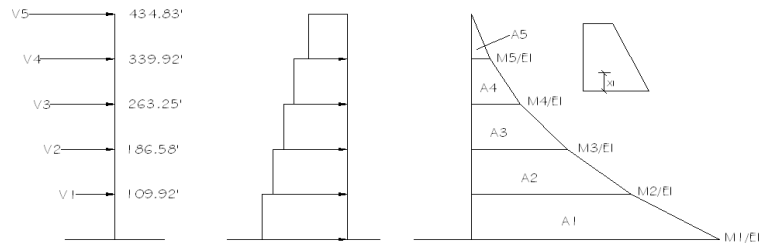


Figure 28: Load, Shear and Moment Relationship of Moment Area Method

The structure was split into five groups, 8 stories to each group. The wind forces were summed up for each group and were said to act at the top story of each design group. From the winds loads, a shear and moment relationship can be developed as shown in Figure 28. Dividing the moments by the unknown EI, the areas of each piece of the M/EI diagram can be found by

$$A_i = ((M_i + M_{i+1}) \times h_i) \div (2EI_{oi}) \quad \text{Equation 1}$$

Where $E = 29000\text{ksi}$ for steel and I is the end column moment of inertia found by

$$I_{oi} = \Sigma(A_{ci}d_i^2) \quad \text{Equation 2}$$

Where d is the center line to center line distance between the end columns and A_{ci} is the gross area of the end columns. With the target deflection set to $H/400$ in both the E-W and N-S direction, this value can be substituted into Equation 6, leaving only the required moment of inertia for each design group as the unknown. By substituting the distances squared and rearranging Equation 4, the areas of the columns of each design group can be found. These required areas are summarized in Figure 29 below.

$$\bar{X}_i = \frac{h_i}{3} \left(\frac{M_i + 2M_{i+1}}{M_i + M_{i+1}} \right) \quad \text{Equation 5}$$

$$\Delta_{ci} = A_i(h_i - \bar{X}_i) + \sum_{j=1}^{i-1} A_j (H_i - \bar{X}_j) \quad \text{Equation 6}$$



Overturning Moment			Required Column Area		
M5	1542667.1	in-kips	Acol5	22.439	in ²
M4	3585800	in-kips	Acol4	68.5828	in ²
M3	5985908.3	in-kips	Acol3	143.528	in ²
M2	8762778.8	in-kips	Acol2	252.781	in ²
M1	12955479	in-kips	Acol1	424.176	in ²

Figure 29: Moment Area Method Column Area Summary

Because the area of a W14x730, the largest W-shape column available in today's steel market, is 215in^2 , built-up or composite column sections are required. After speaking with Malcolm Bland, principal at The Harman Group, it was found that built-up sections are typically preferred over composite column sections because of construction management issues, including sequencing and constructability of connections. The design sections of these built-up columns will be discussed later in this section of the report.

Classical Virtual Work Method (as presented in AISC Design Guide 5)

As moment area method is a great tool to obtain initial braced frame column sizes, a method is needed to find initial sizes of braces and girders. The method chosen is the classical virtual work method presented in AISC Design Guide 5. This is an optimization method utilized for "inverted V" or "chevron" braced frames. Final member sizes are obtained by multiplying required areas by a correction factor that accounts for drift. This method can be found complete in Appendix C.

Many assumptions had to be made in order to use this method. The geometry of all bays in the braced frames had to be assumed to be concentric inverted "V", when in reality some eccentric braces exist. Because of this assumption, these calculations will approximate a drift that is much smaller than the actual drift. As with moment area method, all braced frames were assumed to contribute equally to lateral force resistance.

The procedure to find optimal member areas involves first finding member forces due to the external wind forces; second finding member forces due to virtually applied forces at the point deflection is to be optimized; third calculating areas due to strain with $\lambda = 1.0$; fourth computing the deflection by virtual loads with $\lambda = 1.0$; and finally applying a correction factor which is the ratio of the target deflection of $H/400$ to the calculated deflection. The results of this method are summarized below in Figure 30. The column sizes of classical virtual work method are compared to that of the moment area method. The member areas required are fairly similar to each other; classical virtual work shows the requirement of a larger column area.



	Classic Virtual Work			Moment Area Method	
	A_{col}	A_{brace}	A_{girder}	Ovt Mom	A_{col}
Group 5	76.226206	9.32948	11.7558	1542667.1	22.4390097
Group 4	178.98679	11.9457	15.0525	3585800	68.5828473
Group 3	288.64802	13.5319	17.0512	5985908.3	143.527923
Group 2	380.54798	14.3852	18.1264	8762778.8	252.781058
Group 1	498.74328	14.8786	24.1676	12955479	424.176461

Figure 30: Classical Virtual Work Summary with Comparison to Moment Area Method

ETABS Frame Analysis

ETABS was chosen for the lateral analysis software of choice for this study due to its proven use in the design of the world's tallest and most complex structures. The floor plans and story heights of the Trump Taj Mahal Hotel tower were entered into the model. 2 models were created; a model for drift and a model for strength. The strength model will be discussed later in this report. The drift model assumes rigid diaphragm action of the precast concrete plank floor system. The mass of each floor was lumped per unit area of the diaphragm; this mass was obtained from the RAM Steel gravity model output. The wind loads from the wind tunnel test were input into the model; all 20 of the cases were considered. For drift design, a 25% reduction was applied to these wind loads as a way of converting a 50 year wind speed (strength) to a 10 year wind speed (serviceability). A minimum 25% reduction was recommended by AISC Design Guide 3 and ASCE 7-05 Commentary on Wind Loads (Chapter 6). Tabulated seismic loads per AISC 7-05 Equivalent Lateral Force Procedure were also imposed on the structure in both the north/south and east/west directions; a $\pm 5\%$ accidental torsion was applied to the structure. For clarity, the following table list all load cases input into ETABS with a brief description of each.

Dead	Self Weight and Superimposed Dead Loads
Live	Live Load per ASCE 7-05 Requirements
Wind1 - 20	Wind Tunnel Test Wind Load Case, 20 Cases Total – Drift Model has 25% Reduction Applied per AISC Design Guide 3.
EQX	Seismic Forces Acting East/West
EQXE1	Seismic Forces Acting East/West with +5% Accidental Eccentricity
EQXE2	Seismic Forces Acting East/West with -5% Accidental Eccentricity
EQX	Seismic Forces Acting North/South
EQXE1	Seismic Forces Acting North/South with +5% Accidental Eccentricity
EQXE2	Seismic Forces Acting North/South with -5% Accidental Eccentricity

Table 4: ETABS Load Case Identification

The braced frame cores were constrained geometrically to allow space for the required openings of the redesigned service core. Although it is preferred to have all concentric braced frames, eccentric braced frames were required in Braced Frame 1 (E-W direction) in order to accommodate the openings into the elevator lobby. The elevations of the 8 braced frames are shown in Figure 31 below (See Figure 25 for plan layout of braced frames). 5 design groups were created for the columns, braces and girders; each



design group encompassing 8 stories of the braced frames. Concentric and eccentric braced frames were put into 2 different design groups because of the differing behavior of each.

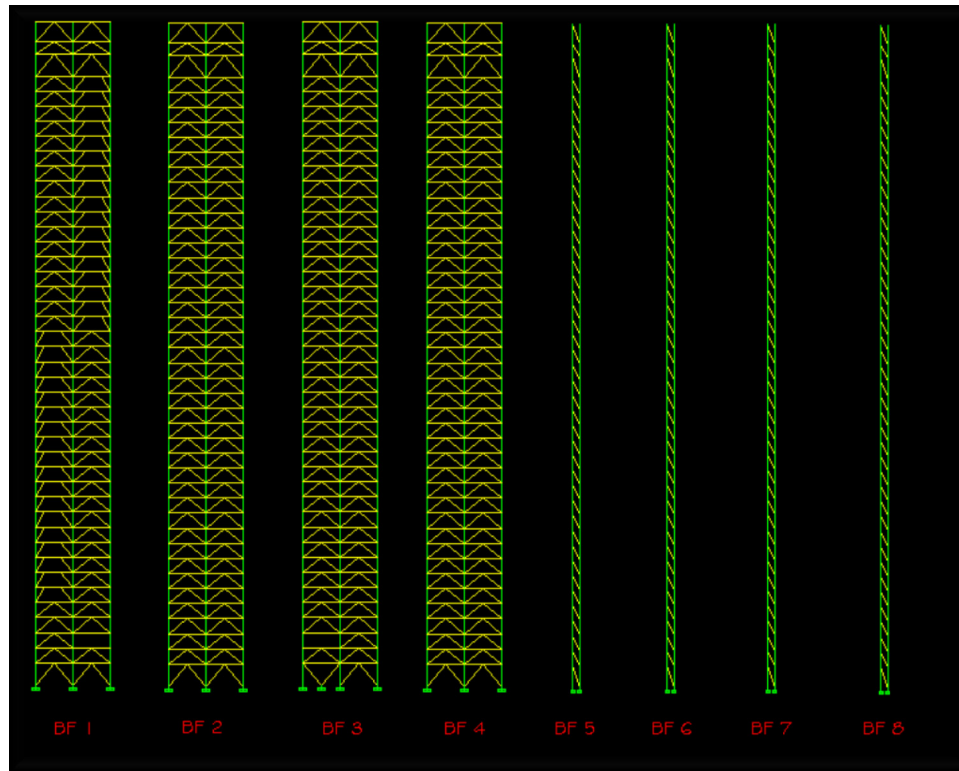


Figure 31: Braced Frame Elevations

Initial member sizes determined by classical virtual work method and moment area method were input into the model. The model was run with P-delta effects considered. Iterations were performed on the member sizes of each of the 5 design groups until the drift limitation of $H/400$ was met and member optimization was accomplished.

After completing the drift optimization of the frames, a strength model was created. This model differs from the drift model in that semi-rigid diaphragms were assumed in order to impose axial forces on the girders of the braced frames. “Dummy” null areas acting as tributary areas were also setup up around the braced frames to distribute floor dead and live loads onto the braced frame members (See Figure 32). The full wind tunnel test wind loads were used for strength design.

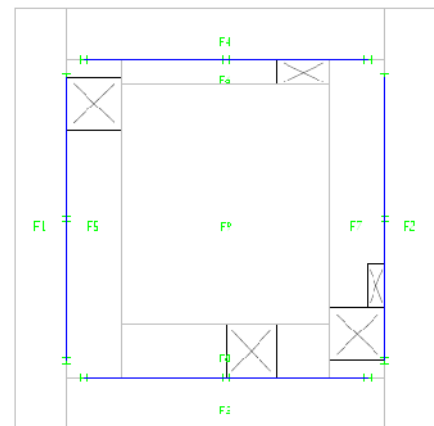


Figure 32: “Dummy” Null Tributary Areas



For LRFD, the load combinations of ASCE 7-05 Chapter 2 Strength Design were used to obtain the ultimate design loads of the structure. The load combinations are as follows:

1. $1.2D + 1.6L + 0.5(L_r \text{ or } S \text{ or } R)$
2. $1.2D + 1.6(L_r \text{ or } S \text{ or } R) + (L \text{ or } 0.80W)$
3. $1.2D \pm 1.6W + L + 0.5((L_r \text{ or } S \text{ or } R))$
4. $1.2D \pm 1.0E + L + 0.2S$
5. $0.90D \pm 1.6W$
6. $0.90D \pm 1.0E$

*Note: \pm indicates the possibility of uplift resulting from lateral forces

Overall, ultimate member forces were compared and designed to meet equation H1-1a (Equation 5) or H1-1b (Equation 6), members under combined forces, as specified in Chapter H of AISC Manual of Steel Construction 13th Edition. As shown below, the interaction equation must not exceed 1.0.

$$\text{For } \frac{P_r}{P_c} \leq 0.2$$

$$\frac{P_r}{P_c} + \frac{8}{9} \left(\frac{M_{rx}}{M_{cx}} + \frac{M_{ry}}{M_{cy}} \right) \leq 1.0 \quad \text{H1-1a (Equation 3)}$$

$$\text{For } \frac{P_r}{P_c} > 0.2$$

$$\frac{P_r}{2P_c} + \left(\frac{M_{rx}}{M_{cx}} + \frac{M_{ry}}{M_{cy}} \right) \leq 1.0 \quad \text{H1-1b (Equation 4)}$$

Iterations were performed until the interaction equation of all members did not exceed 1.0. Braced Frame elevations complete with interaction ratios can be seen in Figure 33. Please note that all red members are extremely close to 1.0, but do not exceed it. Any increases in member sizes due to strength requirements were updated in the drift model; the drift model was re-run with these updated member sizes. A schedule of the final member sizes of each braced frame can be found in Figure 34. The section properties of built-up column sections can be found in Figure 35.

Spot checks of columns, braces, and girders were performed to verify the design outputs of ETABS. These spot checks were performed by superimposing the gravity loads obtained from RAM Steel on the columns and girders. These loads were then input into a spreadsheet with the member's design section in order to determine conformance with Equation 7 and Equation 8. Brace designs were spot checked on the basis of limiting slenderness ratios to $KL/r \leq 300$ for tension and $KL/r \leq 200$ for compression. Calculations and spot checks are available upon request.



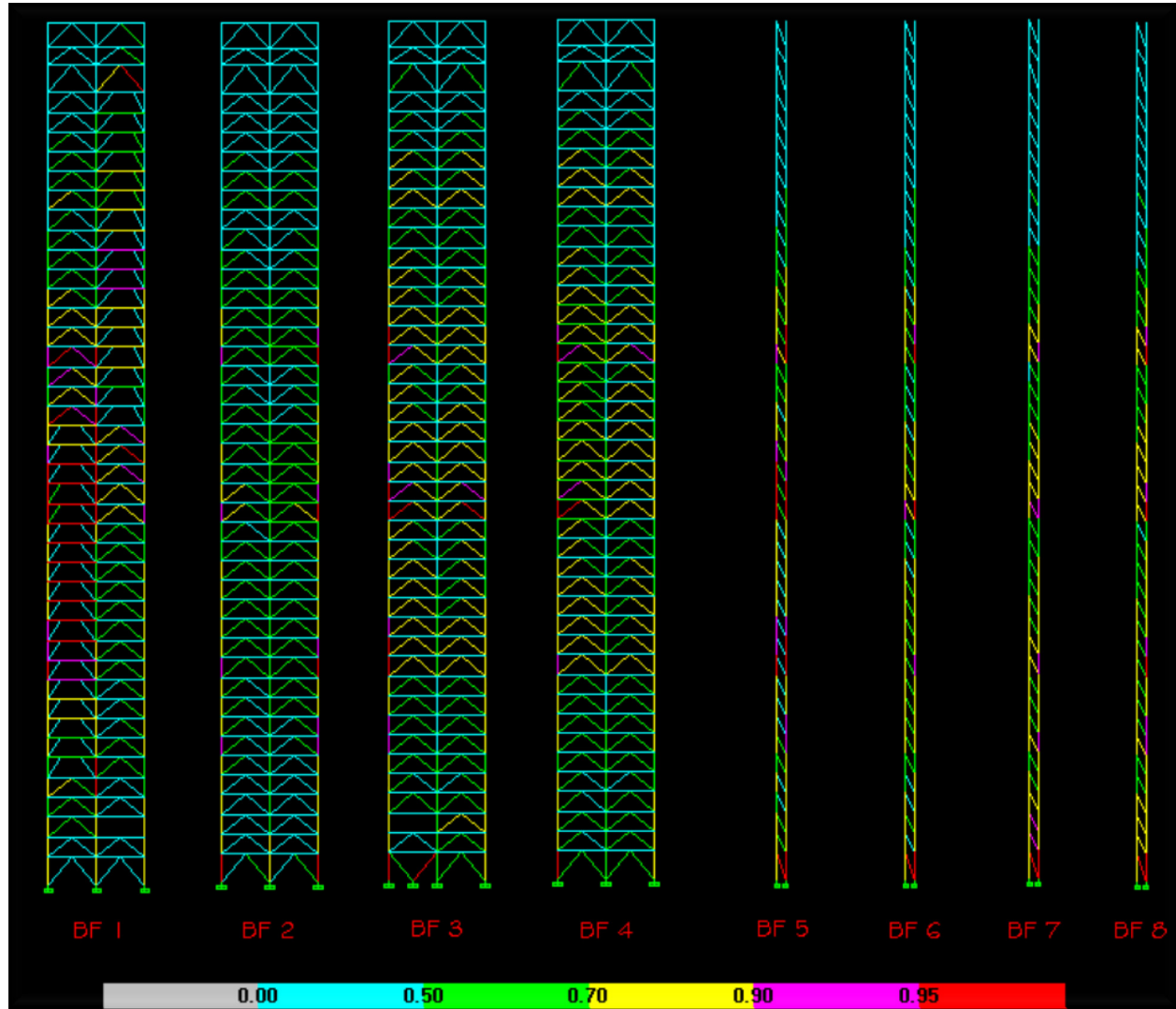


Figure 33: Braced Frame Strength Design – Interaction Equations

Having both the strength and drift models finalized, output can now be processed and used for comparison purposes. For the purpose of this study, it is important to compare the performance of the braced frame core to that of the concrete shear wall core. Please note that all of the results used for the concrete shear wall core are taken from the analyses and investigations completed in Technical Report Number 3 (Reichwein, December 2007). Figure 36 and Figure 37 compare the center of rigidity and inherent eccentricity of both the concrete shear wall and braced frame core. It is important to note that the braced frame core was designed in such a way to minimize the inherent torsion of the structure. This involved an architectural redesign of the service core which was not considered for the concrete shear wall core. By comparison, the concrete shear wall core exhibits much more inherent eccentricity as compared to the braced frame core.



Braced Frame Schedule

Concentrically Braced Frames (BF 1,2,3,4)			
Levels	Column	Brace	Girder
1 - 4	Builtup 3	W12x210	W14x132
5 - 8	Builtup 2	W12x170	W14x132
9 - 16	Builtup 1	W12x136	W14x109
17 - 24	W14x550	W12x106	W16x89
25 - 32	W14x311	W12x87	W16x77
33 - Roof	W14x257	W12x53	W16x77

Eccentrically Braced Frames (BF 1 Only)			
Levels	Column	Brace	Girder
3 - 4	Builtup 3	W12x210	W14x145
5 - 8	Builtup 2	W12x170	W14x145
9 - 16	Builtup 1	W12x136	W14x145
17 - 24	W14x550	W12x106	W14x120
25 - 32	W14x311	W12x87	W16x77
33 - 38	W14x257	W12x53	W16x77

BF 5,6,7,8	
Levels	Brace
1 - 16	2L8x8x1
16 - Roof	2L6x6x1

Figure 34: Braced Frame Column, Brace, and Girder Schedule

Built-up Column Section Properties

Section	Wt (plf)	A (in ²)	I ₃₃ (in ⁴)	I ₂₂ (in ⁴)	S ₃₃ (in ³)	S ₂₂ (in ³)	z ₃₃ (in ³)	z ₂₂ (in ³)	r ₃₃ (in)	r ₂₂ (in)
Builtup 1	908.54	267	22048	5465	1694	611	2292	986	9	4.5
Builtup 2	1112.71	327	33964	6550	2235	732	3137	1208	10.2	4.5
Builtup 3	1429.17	420	42840	12125	2856	1212	3960	1875	10.1	5.3

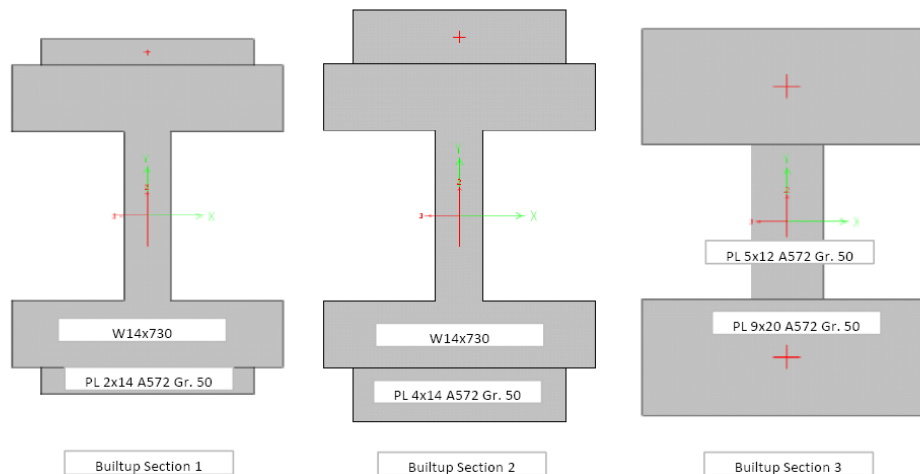


Figure 35: Built-up Column Section Properties



Braced Frame Core							Shear Wall Core						
Story	XCM	YCM	XCR	YCR	%eX	%eY	Story	XCM	YCM	XCR	YCR	%eX	%eY
STORY40	804.44	797.22	793.50	963.39	1.36	20.84	STORY40	347.56	347.65	522.75	638.71	50.41	83.72
STORY39.1	800.88	801.03	793.63	973.66	0.91	21.55	STORY39	347.26	347.46	523.96	641.33	50.88	84.58
STORY39	802.08	799.81	793.72	980.76	1.04	22.62	STORY38	346.40	346.00	526.12	638.43	51.88	84.52
STORY38	802.06	799.86	793.95	994.36	1.01	24.32	STORY37	346.39	346.00	527.80	635.43	52.37	83.65
STORY37	802.05	799.89	794.70	994.76	0.92	24.36	STORY36	346.39	346.00	529.67	631.50	52.91	82.52
STORY36	802.05	799.89	795.67	994.26	0.80	24.30	STORY35	346.39	346.00	531.75	626.77	53.51	81.15
STORY35	802.05	799.89	796.79	993.39	0.66	24.19	STORY34	346.39	346.00	534.06	621.37	54.18	79.59
STORY34	802.05	799.89	798.05	992.22	0.50	24.04	STORY33	346.39	346.00	536.64	615.40	54.92	77.86
STORY33	802.05	799.89	799.44	990.86	0.32	23.88	STORY32	346.39	346.00	539.53	608.99	55.76	76.01
STORY32	802.03	799.92	800.96	989.25	0.13	23.67	STORY31	346.39	346.00	542.76	602.27	56.69	74.07
STORY31	802.02	799.94	802.60	985.28	0.07	23.17	STORY30	346.39	346.00	546.37	595.37	57.73	72.07
STORY30	802.02	799.94	804.29	981.57	0.28	22.71	STORY29	346.39	346.00	550.41	588.47	58.90	70.08
STORY29	802.02	799.94	806.01	978.29	0.50	22.29	STORY28	346.39	346.00	554.92	581.76	60.20	68.14
STORY28	802.02	799.94	807.76	975.59	0.72	21.96	STORY27	346.39	346.00	559.96	575.47	61.65	66.32
STORY27	802.02	799.94	809.53	973.71	0.94	21.72	STORY26	346.39	346.00	565.55	569.82	63.27	64.69
STORY26	802.02	799.94	811.31	972.93	1.16	21.62	STORY25	346.39	346.00	571.76	565.09	65.06	63.32
STORY25	802.02	799.94	813.07	973.62	1.38	21.71	STORY24	346.39	346.00	578.62	561.53	67.04	62.29
STORY24	802.00	799.97	814.77	976.18	1.59	22.03	STORY23	346.39	346.00	586.20	559.38	69.23	61.67
STORY23	801.98	800.00	816.23	980.11	1.78	22.51	STORY22	346.39	346.00	594.63	559.14	71.67	61.60
STORY22	801.98	800.00	817.46	987.10	1.93	23.39	STORY21	346.36	346.73	603.38	560.44	74.21	61.63
STORY21	802.03	800.00	818.38	996.23	2.04	24.53	STORY20	347.57	346.45	620.08	556.95	78.41	60.76
STORY20	802.11	800.00	818.41	994.86	2.03	24.36	STORY19	346.62	346.28	624.70	557.91	80.23	61.11
STORY19	802.11	800.00	818.33	991.47	2.02	23.93	STORY18	346.62	346.28	626.21	558.42	80.66	61.26
STORY18	802.11	800.00	818.23	987.14	2.01	23.39	STORY17	346.62	346.28	626.21	558.57	80.37	61.30
STORY17	802.11	800.00	818.09	981.80	1.99	22.73	STORY16	346.62	346.28	622.11	558.46	79.48	61.27
STORY16	802.10	800.02	817.89	975.29	1.97	21.91	STORY15	346.62	346.28	617.19	558.12	78.06	61.18
STORY15	802.10	800.05	817.51	966.69	1.92	20.83	STORY14	346.62	346.28	610.66	557.53	76.18	61.00
STORY14	802.10	800.05	817.15	958.09	1.88	19.75	STORY13	346.62	346.28	602.61	556.61	73.85	60.74
STORY13	802.10	800.05	816.84	948.98	1.84	18.61	STORY12	346.62	346.28	593.08	555.31	71.11	60.36
STORY12	802.10	800.05	816.60	939.22	1.81	17.39	STORY11	346.62	346.28	582.31	553.90	68.00	59.96
STORY11	802.10	800.05	816.44	928.75	1.79	16.09	STORY10	346.62	346.28	569.35	551.74	64.26	59.33
STORY10	802.10	800.05	816.41	917.46	1.78	14.68	STORY9	346.62	346.28	554.79	548.39	60.06	58.36
STORY9	802.10	800.05	816.58	905.25	1.81	13.15	STORY8	346.62	346.28	538.75	543.99	55.43	57.09
STORY8	802.09	800.08	816.98	891.91	1.86	11.48	STORY7	346.62	346.28	521.13	538.31	50.35	55.45
STORY7	802.10	800.12	817.45	877.00	1.91	9.61	STORY6	346.62	346.28	501.80	530.96	44.77	53.33
STORY6	802.10	800.12	818.35	862.16	2.03	7.76	STORY5	346.62	346.28	480.51	521.39	38.63	50.57
STORY5	802.10	800.12	819.91	847.16	2.22	5.88	STORY4	346.69	346.61	456.70	513.20	31.73	48.06
STORY4	802.09	800.12	822.48	832.10	2.54	4.00	STORY3	333.30	340.56	432.89	529.02	29.88	55.34
STORY3	802.04	800.02	826.32	822.87	3.03	2.86	STORY2	346.85	346.01	318.26	360.11	8.24	4.07
STORY2.1-1	801.97	799.92	831.67	829.88	3.70	3.75	STORY1	350.99	344.85	321.25	290.54	8.47	15.75
STORY2.1	802.32	800.80	833.39	832.81	3.87	4.00							
STORY2	802.33	800.80	805.99	800.17	0.46	0.08							
STORY1	801.96	799.92	807.46	800.83	0.69	0.11							

Figure 36: Center of Mass, Center of Rigidity, and Inherent Eccentricity of Both the Shear Wall and Braced Frame Core

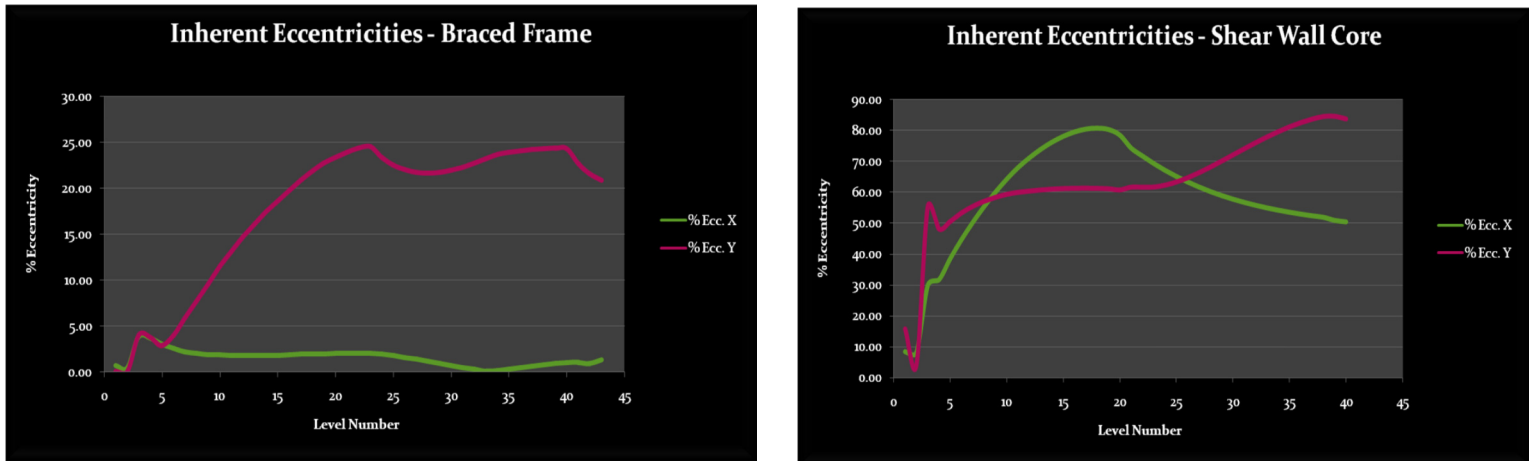


Figure 37: Inherent Eccentricity Comparison of Both Structural Systems



The seismic story drift of the braced frame core under the most severe seismic load case was well under the allowable story height of $0.20 \times h_x$. Results of the seismic story drift are illustrated in Figure 38 and Figure 38 below. The seismic drift of all load cases can be found in Appendix D.

Wind drift governed the design of most members of the braced frame core. A drift limitation of $H/400$ was used as recommended by AISC Design Guide 3 and ASCE 7-05. A comparison of the drift resulting from the most severe wind tunnel test load case of both the concrete shear wall core and the braced frame core is shown below in Figure 39. Figure 40 is a graphic of the comparison of the drift of both systems versus $H/400$ and $H/500$, respectively. As can be seen by both of these figures, the drift of the concrete shear wall core falls below $H/500$ for all levels, whereas the drift of the braced frame core barely meets the limitation of $H/400$. As P-delta effects were considered, Figure 41 illustrates the most severe wind case drift for the braced frame core with and without P-delta effects. P-delta effects had only contributed to a slight increase in overall building drift. All results of the braced frame core drift for all wind tunnel test load cases can be found in Appendix D.

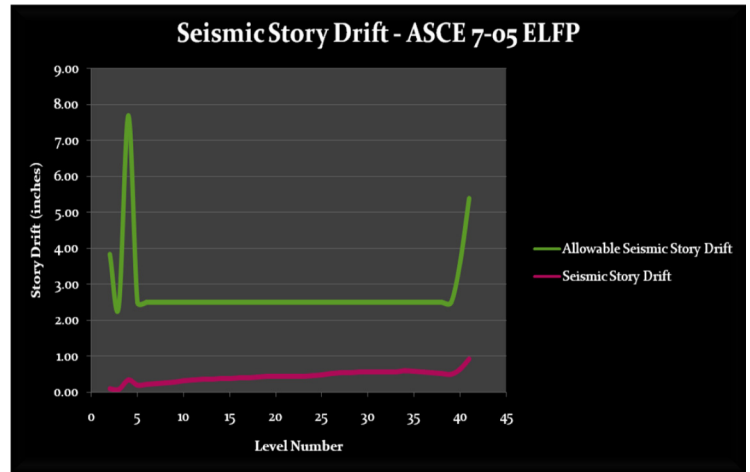


Figure 37: Seismic Story Drift Versus Allowable

Building Drift Under Most Severe Seismic Case (Cd = 3.3)						
Braced Frame Core (EQXE2)						
Level	Height (ft)	Total Drift (in)	Amplified Drift (in)	H/?	Amplified Story Drift (in)	ASCE 7-05 Allowable Story Drift (in)
41	460.00	5.30	17.49	315.64	0.93	5.38
40	437.58	5.02	16.56	317.08	0.64	3.60
39	422.58	4.82	15.92	318.51	0.50	2.50
38	412.17	4.67	15.42	320.78	0.53	2.50
37	401.75	4.51	14.89	323.75	0.55	2.50
36	391.33	4.35	14.34	327.41	0.57	2.50
35	380.92	4.17	13.78	331.81	0.58	2.50
34	370.50	4.00	13.19	337.00	0.59	2.50
33	360.08	3.82	12.60	342.94	0.56	2.50
32	349.67	3.65	12.04	348.65	0.57	2.50
31	339.25	3.48	11.47	354.95	0.57	2.50
30	328.83	3.30	10.90	361.94	0.56	2.50
29	318.42	3.13	10.34	369.62	0.56	2.50
28	308.00	2.96	9.78	377.96	0.55	2.50
27	297.58	2.80	9.23	386.91	0.54	2.50
26	287.17	2.63	8.69	396.37	0.52	2.50
25	276.75	2.48	8.18	406.05	0.48	2.50
24	266.33	2.33	7.70	415.07	0.46	2.50
23	255.92	2.19	7.24	424.01	0.44	2.50
22	245.50	2.06	6.81	432.80	0.43	2.50
21	235.08	1.93	6.38	442.47	0.44	2.50
20	224.67	1.80	5.94	453.92	0.44	2.50
19	214.25	1.67	5.50	467.31	0.44	2.50
18	203.83	1.54	5.07	482.81	0.43	2.50
17	193.42	1.41	4.64	500.45	0.41	2.50
16	183.00	1.28	4.23	518.95	0.40	2.50
15	172.58	1.16	3.84	539.85	0.39	2.50
14	162.17	1.05	3.45	564.09	0.38	2.50
13	151.75	0.93	3.07	592.40	0.36	2.50
12	141.33	0.82	2.71	625.69	0.35	2.50
11	130.92	0.72	2.36	665.26	0.33	2.50
10	120.50	0.61	2.03	712.84	0.31	2.50
9	110.08	0.52	1.72	769.96	0.28	2.50
8	99.67	0.43	1.44	833.35	0.26	2.50
7	89.25	0.36	1.17	911.64	0.24	2.50
6	78.83	0.28	0.93	1012.24	0.22	2.50
5	68.42	0.22	0.72	1147.02	0.19	2.50
4	58.00	0.16	0.53	1323.14	0.35	7.68
3	26.00	0.05	0.18	1747.61	0.08	2.40
2	16.00	0.03	0.10	1945.88	0.10	3.84

Figure 38: Seismic Story Drift



Building Drift Comparison Under Most Severe Wind Tunnel Case (P-Delta Effects and 25% Reduction)										
Level	Shear Wall Core (Case 12)				Braced Frame Core (Case 9)				Drift Ratios	
	Height (ft)	Total Drift (in)	H/?	Story Drift (in)	Height (ft)	Total Drift (in)	H/?	Story Drift (in)	H/400 (in)	H/500 (in)
41	434.83	7.77	671.98	0.34	460.00	12.87	428.98	0.81	13.80	11.04
40	407.00	7.43	657.69	0.24	437.58	12.06	435.45	0.56	13.13	10.50
39	397.42	7.18	663.75	0.16	422.58	11.50	441.12	0.40	12.68	10.14
38	387.83	7.02	662.75	0.17	412.17	11.10	445.56	0.40	12.37	9.89
37	378.25	6.85	662.18	0.17	401.75	10.70	450.65	0.41	12.05	9.64
36	368.67	6.68	662.09	0.18	391.33	10.29	456.49	0.42	11.74	9.39
35	359.08	6.50	662.44	0.18	380.92	9.87	463.13	0.42	11.43	9.14
34	349.50	6.32	663.27	0.19	370.50	9.45	470.66	0.43	11.12	8.89
33	339.92	6.14	664.57	0.19	360.08	9.02	479.05	0.40	10.80	8.64
32	330.33	5.95	666.32	0.19	349.67	8.62	486.85	0.40	10.49	8.39
31	320.75	5.76	668.52	0.19	339.25	8.22	495.36	0.40	10.18	8.14
30	311.17	5.56	671.16	0.20	328.83	7.82	504.71	0.40	9.86	7.89
29	301.58	5.37	674.22	0.20	318.42	7.42	514.93	0.39	9.55	7.64
28	292.00	5.17	677.64	0.20	308.00	7.03	526.07	0.39	9.24	7.39
27	282.42	4.97	681.36	0.20	297.58	6.64	538.18	0.38	8.93	7.14
26	272.83	4.78	685.28	0.19	287.17	6.25	551.30	0.38	8.62	6.89
25	263.25	4.58	689.24	0.19	276.75	5.87	565.36	0.36	8.30	6.64
24	253.67	4.39	693.00	0.19	266.33	5.52	579.18	0.35	7.99	6.39
23	244.08	4.21	696.27	0.18	255.92	5.17	594.20	0.34	7.68	6.14
22	234.50	4.03	698.25	0.15	245.50	4.82	610.58	0.34	7.37	5.89
21	224.92	3.88	695.40	0.19	235.08	4.49	628.40	0.33	7.05	5.64
20	215.33	3.70	699.23	0.20	224.67	4.16	647.75	0.32	6.74	5.39
19	205.75	3.50	706.13	0.21	214.25	3.84	668.75	0.31	6.43	5.14
18	196.17	3.29	715.81	0.21	203.83	3.54	691.55	0.30	6.11	4.89
17	186.58	3.07	728.41	0.22	193.42	3.24	715.96	0.27	5.80	4.64
16	177.00	2.85	744.14	0.22	183.00	2.97	739.82	0.27	5.49	4.39
15	167.42	2.63	763.24	0.22	172.58	2.70	766.16	0.26	5.18	4.14
14	157.83	2.41	786.09	0.22	162.17	2.45	795.55	0.25	4.87	3.89
13	148.25	2.19	813.22	0.22	151.75	2.20	828.52	0.24	4.55	3.64
12	138.67	1.97	845.18	0.21	141.33	1.96	865.66	0.23	4.24	3.39
11	129.08	1.76	882.07	0.21	130.92	1.73	907.68	0.22	3.93	3.14
10	119.50	1.55	925.88	0.20	120.50	1.51	955.65	0.20	3.62	2.89
9	109.92	1.35	978.49	0.19	110.08	1.31	1009.55	0.18	3.30	2.64
8	100.33	1.16	1042.33	0.18	99.67	1.13	1060.76	0.17	2.99	2.39
7	90.75	0.97	1120.83	0.17	89.25	0.96	1117.49	0.16	2.68	2.14
6	81.17	0.80	1218.57	0.16	78.83	0.80	1181.90	0.15	2.36	1.89
5	71.58	0.64	1342.19	0.14	68.42	0.65	1255.17	0.14	2.05	1.64
4	62.00	0.50	1490.68	0.41	58.00	0.52	1341.04	0.33	1.74	1.39
3	26.00	0.09	3545.45	0.05	26.00	0.19	1666.67	0.08	0.78	0.62
2	16.00	0.04	5026.18	0.04	16.00	0.11	1789.38	0.11	0.48	0.38

Figure 39: Building Drift of Both Systems Resulting from the Most Severe Wind Tunnel Load Case



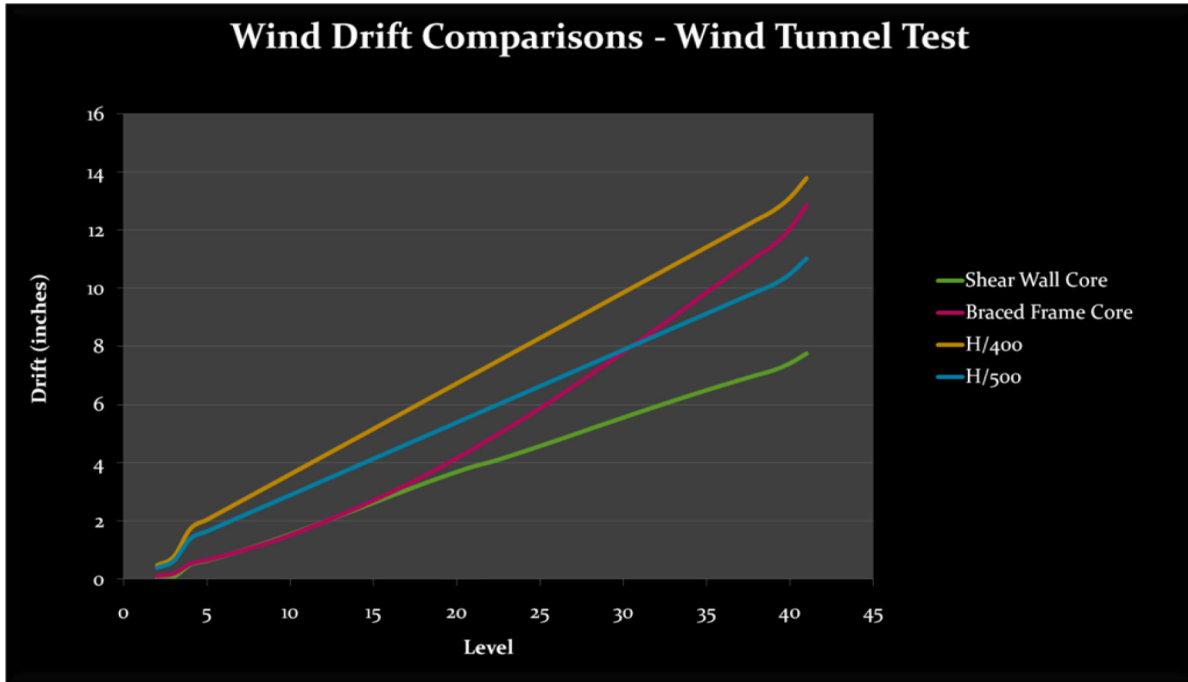


Figure 40: Wind Drift Comparison of Both Systems versus H/400 and H/500

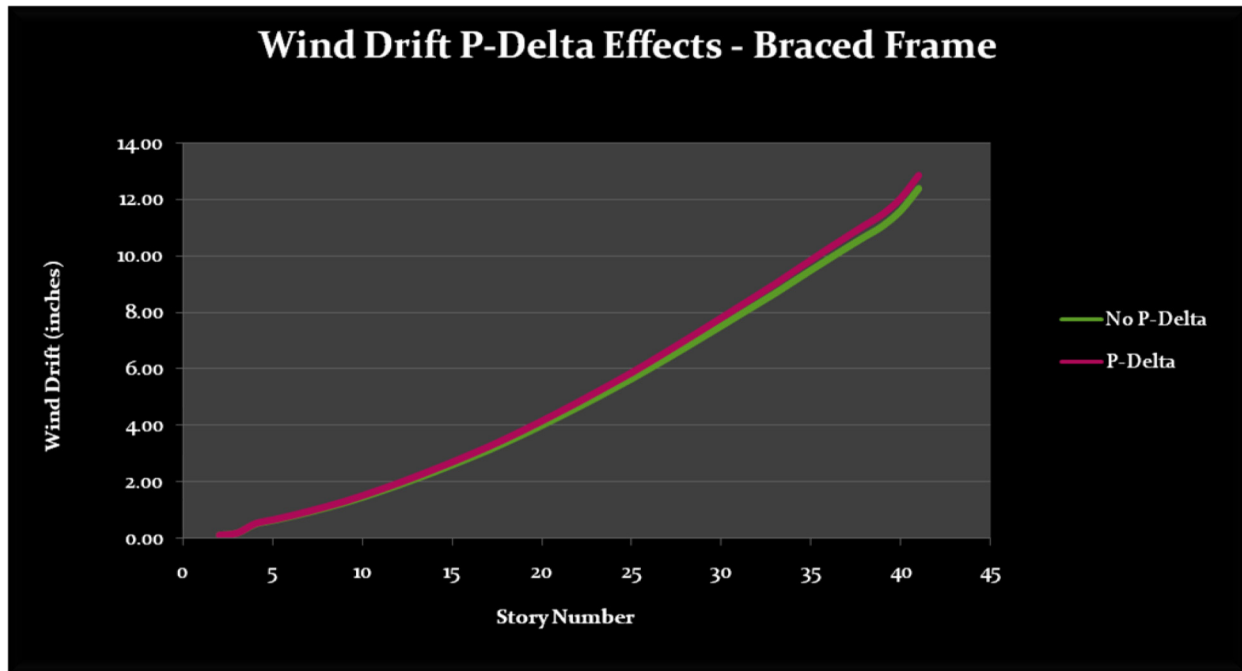


Figure 41: P-Delta Effects on the Braced Frame Core



Braced Frame Connection Design and Detailing

An important aspect of the investigation of converting a concrete structure to a steel structure is the effect on the floor to floor height. While detailing the braced frame connections it was found that a minimum 10" increase, 30'-0" total building height increase is required to accommodate the braced frame connections without impeding core openings. However, a simple gusset plate that acts as at the interface of the brace and girder would require an even larger increase in floor to floor height as to not interfere with openings. With the working points taken at the centerline intersections of all members of the braced frame, a special "V" shaped connection is utilized at the brace to girder interface. This "V" shaped connection is comprised of two halves of an ordinary gusset plate shop welded to the bottom flange of the girder; two field bolted plates on each side of the brace act as the connecting element between the brace and gusset plate. A simpler connection is utilized at the brace to column interface. A gusset plate that uses "claw angles" as the connecting element between the gusset plate and brace is utilized at the brace to column interface; the gusset plates are to be shop welded to the column and field bolted to the girder. The entire braced frame connection detail can be seen in Figure 42.

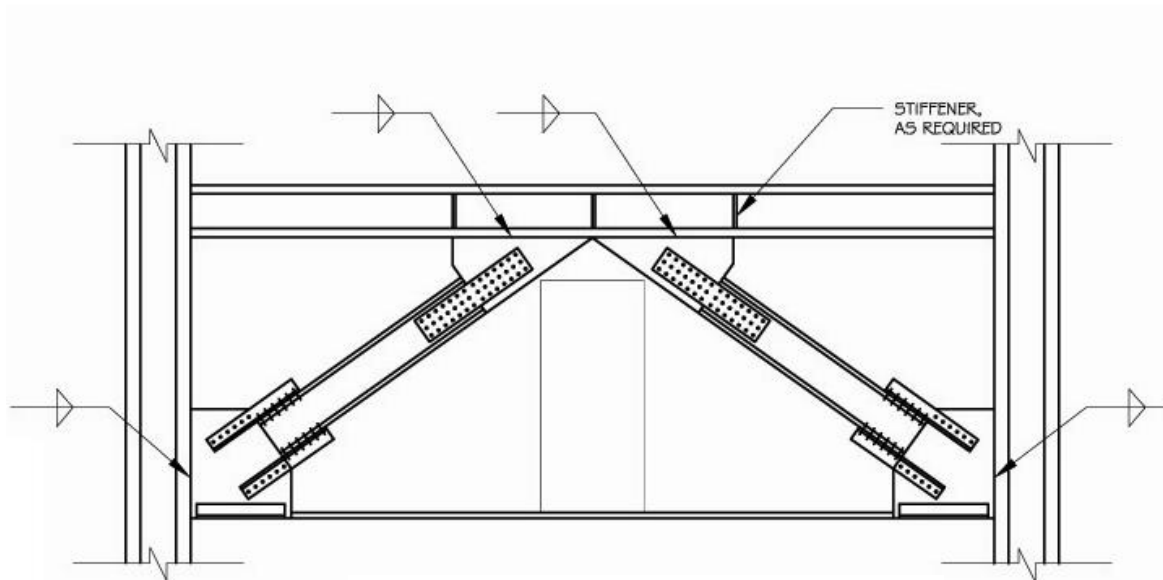


Figure 42: Typical Braced Frame Detail

The design of the braced frame connection was conducted for 5 different axial loads; 1000kip, 800kip, 600kip, 400kip, and 200kip axial forces were considered. It was found that the brace to girder connection was controlled mainly by block shear of the brace W-Shape. Because block shear controls for a 1000kip axial load acting on the largest W14 brace used for the entire braced frame core, higher axial forces will require web reinforcement (such as a welded doubler plate) to accommodate block shear. The girders may also require stiffeners at the brace to girder connection to accommodate flange crippling due to concentrated point loads.



Based on load path analysis, the following limit states were considered for the braced frame connection:

- Brace Limit States
 - Tension Yielding
 - Tension Rupture
 - Block Shear
- Bolt Limit States
 - Bolt Shear
 - Bolt Bearing
 - Brace
 - Plate
 - Gusset Plate
 - Bolt Tearout
 - Brace
 - Plate
 - Gusset Plate
- Gusset Plate Limit states
 - Tension Yielding
 - Tension Rupture
 - Block Shear
 - Compression Buckling
- Weld Limit States
 - Base Metal
 - Weld Rupture

A summary of the connection design is shown below in Table 5 and Table 6 for brace to girder connections and brace to column connections, respectively. The detailed calculations can be found in Appendix E.

Factored Load	Number Rows of Bolts	Bolts Per Row	Plate Thickness, Each (in)	Brace to Gusset Plate Width, each (in)	Gusset Plate Thickness	Weld Size per 1/16"/Weld Length (in)
801kips to 1000kips	4	7	2.25	9	3	8/38
601kips to 800kips	3	7	2	9	2.5	8/30
401kips to 600kips	2	8	1.25	9	1.5	8/22
201kips to 400kips	2	6	0.75	9	1.5	5/24
Up to 200kips	2	5	0.5	9	0.5	5/12

*Table 5: Summary of Brace to Girder Connections
 Note: Plate Fy=36ksi, Bolt Diameter = 3/4", Fillet Welds*



Factored Load	Number Rows of Bolts per Angle	Number of Bolts per Row	Angle Size	Gusset Plate Thickness (inches)
801kips to 1000kips	1	5	L5x5x7/8	1.5
601kips to 800kips	1	4	L5x5x3/4	1.25
401kips to 600kips	1	3	L5x5x3/4	1
201kips to 400kips	1	4	L4x4x7/16	0.625
Up to 200kips	1	3	L3x3x5/16	0.5

*Table 6: Summary of Brace to Column Connections
Note: Plate Fy=36ksi, Bolt Diameter = 3/4"*

Comparatively, the brace to column connection is much more efficient in terms of weight of material used. The limit states of block shear, tension rupture, and tension yielding is often alleviated by claw angles because the thicker flange of the W-Shape is utilized as resistance.

Base Plate Design and Mat Foundation Punching Shear Check

Using the most severe axial load and moment combination of the braced frame core, a base plate was designed to accommodate all of the columns of the braced frame core. As the bases were assumed to be fixed because of the rigidity provided by the mat foundation, the base plates had both a large moment and large axial force acting on them. The base plate was designed in accordance with the LRFD procedure of AISC Design Guide 1 – Base Plate and Anchor Rod Design. RAM Base Plate was utilized to verify the design. The specifications of the base plate are as follows:

- Plate Thickness.....10-1/2"
- Plate Length.....65"
- Plate Width.....55"
- Number of 2-3/4" A449 Grade 120 Anchor Bolts.....32

The overall specification would be an A36 PL 65x55x10.50 with (32) 2-3/4" A449 Grade 120 Anchor Bolts. This is an extremely large plate, comparable to the base plates used at the World Trade Center twin towers. Calculations and details are available upon request.

With a known base plate size, the punching shear of the mat foundation can be checked to verify that a thicker mat will not be required. For punching shear of a rectangular base plate with an aspect ratio of less than 1.5:1.0:

$$V_u \leq \phi V_c = 0.75 \times 4 \times \sqrt{f'_c} \times b_o \times d \quad \text{Equation 5}$$

With V_u equal to 15,910kips, it was found that a 110" thick mat would be required to resist punching shear. The mat foundation provided at the core is 9'0" ≈ 110", therefore it will be concluded that the current mat foundation will satisfy the demands of the braced frame core. Calculations are available upon request.



Tall Building Dynamics

Often, the design of the lateral force resisting systems is governed by serviceability requirements such as drift. However, satisfying drift alone does not guarantee adequate acceleration performance under wind loads, especially wind loads in hurricane prone regions along the Atlantic Ocean coastline. Because steel structural frames are extremely light compared to concrete frames, acceleration issues in the form of human perception are often an issue to consider in the preliminary design. However, the determination of such accelerations can only be truly obtained through wind tunnel studies.

Given the nature of this study, a wind tunnel test is out of the question. However, *Serviceability Limit States Under Wind Loading*, by Lawrence G. Griffis, provides an approximate calculation procedure which may be used in preliminary investigations to determine whether or not building accelerations may be an issue under 10 year recurrent wind forces. According to Griffis, the RMS building acceleration can be determined and compared to the following human response spectrum:

Table 5. Traditional Motion Perception (Acceleration) Guidelines (Note 1) 10-year Mean Recurrence Interval				
Occupancy Type	Peak Acceleration (Milli-g)	Root-mean-square (RMS) Acceleration (Milli-g)		
		1 ≤ T < 4 0.25 < f ≤ 1.0 (g _p ≈ 4.0)	4 ≤ T < 10 0.1 < f ≤ 0.25 (g _p ≈ 3.75)	T ≥ 10 f ≤ 0.1 (g _p ≈ 3.5)
Commercial	15–27 Target 21	3.75–6.75 Target 5.25	4.00–7.20 Target 5.60	4.29–7.71 Target 6.00
Residential	10–20 Target 15	2.50–5.00 Target 3.75	2.67–5.33 Target 4.00	2.86–5.71 Target 4.29
Notation: T = period (seconds) f = frequency (hertz) g _p = peak factor NOTE: 1. RMS and peak accelerations listed in this table are the traditional "unofficial" standard applied in U.S. practice based on the author's experience.				

Figure 43: Motion Perception (Acceleration) Response Parameters

To determine the along-wind, across-wind, torsional, and resultant RMS accelerations of a steel structure, the following equations were used:

$$A_D(Z) = C_D(Z) \frac{U_H^{2.74}}{K_D^{0.37} \times \zeta^{0.5} \times M_D^{0.3}} \tag{Equation 6}$$

$$A_L(Z) = C_L(Z) \frac{U_H^{3.54}}{K_L^{0.77} \times \zeta^{0.5} \times M_L^{0.23}} \tag{Equation 7}$$



$$A_{\theta}(Z) = C_{\theta}(Z) \frac{U_H^{1.88}}{K_{\theta}^{-0.06} \times \zeta^{0.5} \times M_{\theta}^{1.06}} \frac{N_{\theta} B}{U_H} \leq 0.25$$

Equation 8

$$A_{\theta}(Z) = C_{\theta}(Z) \frac{U_H^{1.88}}{K_{\theta}^{-0.06} \times \zeta^{0.5} \times M_{\theta}^{1.06}}, \frac{N_{\theta} B}{U_H} \leq 0.25$$

Equation 9

$$A_{\theta}(Z) = C_{\theta}(Z) \frac{U_H^{2.76}}{K_{\theta}^{0.38} \times \zeta^{0.5} \times M_{\theta}^{0.62}}, \frac{N_{\theta} B}{U_H} > 0.25$$

Equation 10

$$C_D(Z) = 0.0116 \times B^{0.26} \times Z$$

Equation 11

$$C_L(Z) = 0.0263 \times B^{-0.54} \times Z$$

Equation 12

$$C_{\theta}(Z) = 0.00341 \times B^{2.12} \times Z, \frac{N_{\theta} B}{U_H} \leq 0.25$$

Equation 13

$$C_{\theta}(Z) = 0.00510 \times B^{1.24} \times Z, \frac{N_{\theta} B}{U_H} > 0.25$$

Equation 14

$$A_R = (A_D^2 + A_L^2 + (B / \sqrt{2} \times A_{\theta})^2)^{0.5}$$

Equation 15

$$K = (2\pi N)^2 \times M$$

Equation 16

Where:

$A_D(Z), A_L(Z), A_{\theta}(Z)$ = along-wind, across-wind, and torsional RMS accelerations at height Z, respectively (meters/sec², radians/sec²)

A_R = resultant RMS acceleration at the corner of the building

U_H = mean hourly 10 year wind speed at the top of the building (meters/sec)

H = building height (meters)

B = plan dimension of square building (meters)

M = generalized mass of the building (kilograms)

N = frequency (hertz) – obtained from ETABS modal analysis

K = generalized stiffness (Newton/meters) = $(2\pi N)^2 \times M$

ζ = damping ratio - taken as 2% as recommended by ASCE Committee on Tall Buildings

The building frequencies of the braced frame core were determined using ETABS modal analysis and are compared to the concrete shear wall core in the following figure:



Direction	Shear Wall Core		Braced Frame Core	
	Period	Frequency	Period	Frequency
X	3.13	0.32	3.78	0.26
Y	2.75	0.36	4.28	0.23
Rz	1.77	0.56	2.9	0.34

Figure 44: ETABS Modal Analysis – Shear Wall Core and Braced Frame Core

After completing the parametric study of RMS building accelerations, it was found that the resultant RMS acceleration of the steel braced frame core structure is approximately 9.4 milli-g's, which exceeds the target value of 4.8 milli-g's for a residential occupancy by a factor of almost 2. The resultant RMS acceleration of the concrete shear wall core and filigree flat plate system is approximately 4.4 milli-g's, which meets the target acceleration limit of 4.5 milli-g's. This indicates that the braced frame core may not perform adequately under wind loads at upper levels, as occupants may perceive movements caused by excessive accelerations. However, final conclusions can only be made based on a wind tunnel study. Calculations of the parametric RMS acceleration study can be found in Appendix F.

Structural Depth Conclusions

The results of the structural redesign conclude that a steel gravity and lateral structural system can be provided as a viable alternative to the cast-in-place concrete structural system of the Trump Taj Mahal Hotel based on strength and drift requirements. It was found that only a 10" increase in floor to floor height, resulting in approximately 30' additional overall, would be required in order to accommodate the steel framed system. Additional costs incurred will be discussed in both the architectural and construction management breadth studies.

An effective non-composite steel frame with a precast concrete plank floor system was designed to replace the filigree flat plate system. The layout of the steel and precast plank system was designed in such a way as to not interrupt the architectural and mechanical layout of a typical hotel room level. However, in order to conceal the steel framing, soffits will be required around the perimeter W-shape girders of the hotel rooms and also around the brace beams that run in between some of the guest rooms. This will have minor architectural implications that will be discussed later on in the architectural breadth study.

A core of braced frames was designed to replace the concrete shear wall core. These braced frames were laid out around the redesigned elevator/service core as to provide adequate space for openings. To accommodate these openings, it was found that a 10" increase in floor to floor height would be required. The braced frames met the strength requirements and recommended drift requirement of H/400. Built-up



column sections were provided in lieu of composite W-shape columns encased in concrete due to constructability issues and ease of schedule (it is important to remember that scheduling and cost takes first priority in this study).

However, drift and strength are not the only determining factors of conceptual design of a high rise structural system. After performing a parametric study of the RMS accelerations of the tower under wind loading, it was found that the resultant acceleration of the building exceeds the allowable as determined based on occupant perception. The magnitude of the hurricane force wind velocities of Atlantic City, New Jersey, at a 10 year reoccurrence level produce building accelerations that may be considered annoying by building occupants on the upper levels of the tower. Supplementary damping devices in the form of tuned mass dampers or tuned liquid column dampers may be required to control the building response to wind loads. If required, a tuned mass damper will add substantial cost, in the realm of \$2 to \$3 million, to the cost of the building.

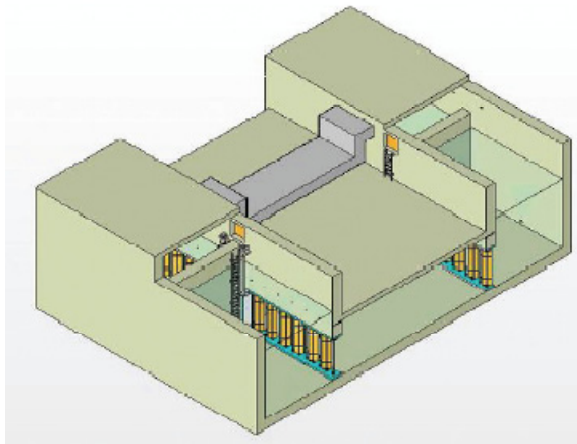


*Figure 46: Tuned Liquid Column Damper
Provided by Motioneering*

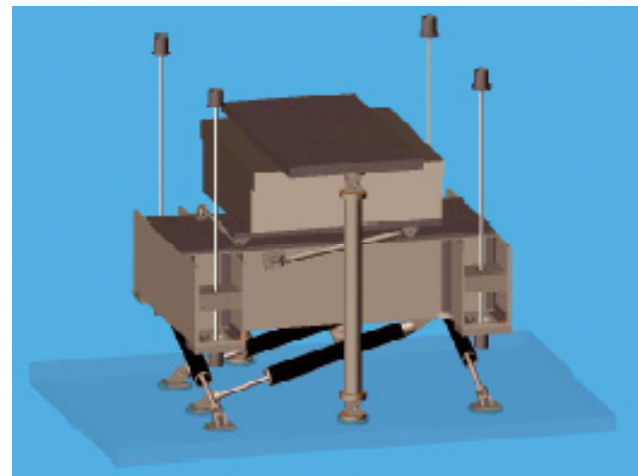


*Figure 45: Tuned Mass Damper, Linked
Provided by Motioneering*

Without the use of a wind tunnel study to adequately determine the actual dynamic properties of the braced frame core and steel structural system, the information presented on the structural redesign indicates acceptable performance on the basis of strength and drift criteria. However, drift and strength are not the only factors of in the design of high-rise structures, as accelerations must be addressed to ensure that human comfort of the building is not an issue. When designing a slender high-rise structure, numerous factors that involve complex analysis of wind forces acting on the structure need to be performed in order to determine the correct structural system for the building type.

